

W -pair production in electron-positron annihilation

R. Philippe

Instituut voor Theoretische Fysica, Universiteit Leuven, B-3030 Leuven, Belgium

(Received 19 February 1982)

The cross section for $e^+e^- \rightarrow W^+W^-$ up to the one-loop level is presented within the framework of quantum flavor dynamics.

I. INTRODUCTION

Presently theoretical and experimental physicists are convinced that the four fundamental forces of nature are adequately described by gauge theories.¹ The self-interactions of the gauge particles are found to play an essential role. Furthermore, the renormalizability of these field theories² allows the calculation of radiative corrections.

At this moment there is very good agreement between quantum flavor dynamics (QFD),³ a non-Abelian gauge theory of electromagnetic and weak interactions based on an $SU_2 \times U_1$ Lie group, and the results of low-energy experiments.

The three-vector-boson vertices of QFD can be studied in detail in the process $e^+e^- \rightarrow W^+W^-$. With the advent of the very-high-energy e^+e^- storage ring LEP at CERN,⁴ this reaction will become experimentally feasible and will undoubtedly provide an important test for the theory.

Therefore, I calculated the cross section for $e^+e^- \rightarrow W^+W^-$ including all one-loop radiative corrections. Results are given in a center-of-mass energy range from 165 up to 500 GeV. Attention is paid to the Higgs-boson-mass dependence of the results. Hard bremsstrahlung is, however, not included because it depends entirely on the accessible phase space, which is different for each experimental setup.

Recently a similar calculation has been done by Lemoine and Veltman,⁵ but I obtain different results. Although the relative behavior of the radiative corrections is quite similar to theirs, there are nevertheless some differences in magnitude, probably due to a different renormalization procedure and to the use of different quark masses.

The outline of my paper is as follows. In Sec. II the model is described. In Sec. III the kinematics is defined. Section IV presents the lowest-order cross section. The one-loop corrections are discussed in Sec. V. Section VI explains the renor-

malization procedure. Bremsstrahlung is treated in Sec. VII. The results are commented upon in Sec. VIII and, finally, conclusions are drawn in Sec. IX.



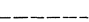
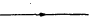


II. MODEL

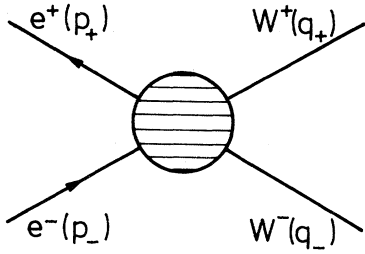
I will briefly describe QFD.³

(i) The theory is based on an $SU_2 \times U_1$ symmetry, which implies the existence of four gauge fields (A_μ , $a = 1, 2, 3$, and B_μ). The corresponding Yang-Mills Lagrangian is given by

$$\mathcal{L}_{\text{YM}} = -\frac{1}{4}F_{\mu\nu}^a F_{\mu\nu}^a - \frac{1}{4}G_{\mu\nu} G_{\mu\nu}$$

TABLE I. Physical and unphysical fields.

Photon γ	A_μ	
Neutral and charged weak vector bosons	Z_μ, W_μ^\pm	
Higgs particle	H	
Leptons and quarks	$\nu_l, l, q_c^1 q_c^\dagger$	
Neutral and charged Higgs-Kibble ghosts	Φ^0, Φ^\pm	
Faddeev-Popov ghosts	Ψ^A, Ψ^0, Ψ^\pm	

FIG. 1. The reaction $e^+e^- \rightarrow W^+W^-$.

with

$$F_{\mu\nu}^a = \partial_\mu A_\nu^a - \partial_\nu A_\mu^a + g\epsilon_{abc}A_\mu^b A_\nu^c,$$

$$G_{\mu\nu} = \partial_\mu B_\nu - \partial_\nu B_\mu.$$

The physical fields, denoted by W_μ^\pm , Z_μ , and A_μ (photon), are related to A_μ^a and B_μ :

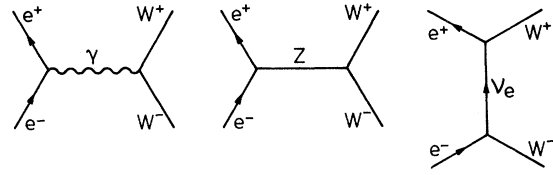
$$W_\mu^\pm = \frac{1}{\sqrt{2}}(A_\mu^1 \mp iA_\mu^2),$$

$$Z_\mu = \cos\theta_W A_\mu^3 - \sin\theta_W B_\mu,$$

$$A_\mu = \sin\theta_W A_\mu^3 + \cos\theta_W B_\mu$$

with θ_W the weak mixing angle.

(ii) In constructing the Lagrangian for the matter fields (leptons ν_l, l and quarks q_c^i, q_c^j), the left-handed fermions are put into SU_2 doublets (f_l), while the right-handed ones are singlets (f_r) under SU_2 . The transformation properties with respect

FIG. 2. The reaction $e^+e^- \rightarrow W^+W^-$ in lowest order.

to U_1 are fixed such that the proper couplings to the photon result.

(iii) The couplings between the vector bosons and the fermions are completely determined by the fact that the covariant derivatives D_μ , involving the gauge fields, acting on f have to transform under $SU_2 \times U_1$ in precisely the same way as f itself.

(iv) A two-component complex scalar field is introduced in order to generate masses for the SU_2 vector bosons and the fermions using the Higgs mechanism.

I performed the calculations in the 't Hooft gauge (in which the vector-boson propagators are diagonal). The complete Lagrangian, including the Faddeev-Popov ghost Lagrangian, is written down in an appendix. The physical and unphysical fields involved are pictorially represented in Table I.

In this paper only two generations of leptons and quarks, each with three color degrees of free-

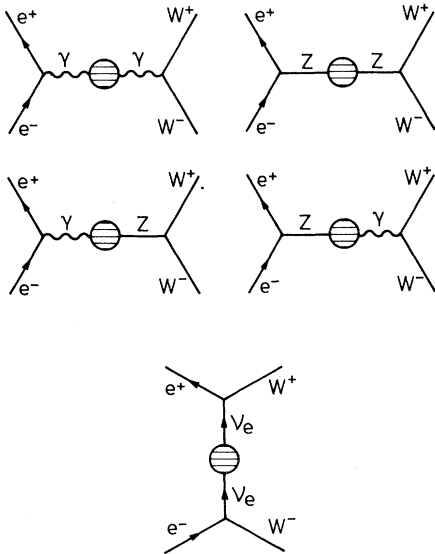
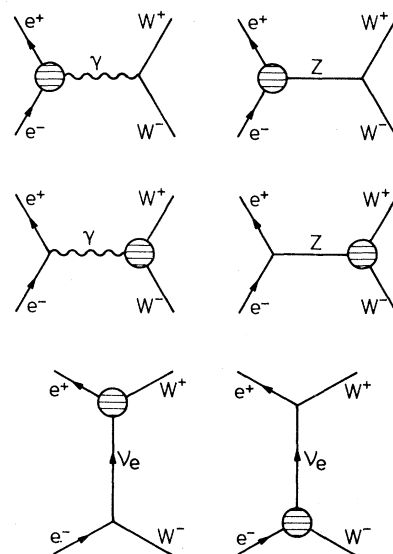
FIG. 3. Self-energy insertions and γZ mixing.

FIG. 4. Vertex corrections.

TABLE II. Self-energy diagrams.

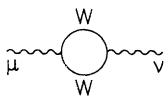
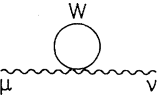
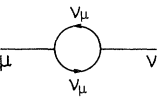
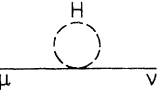
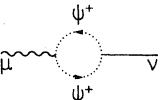
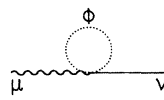
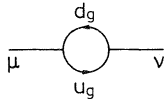
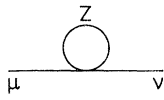
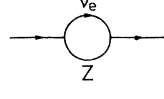
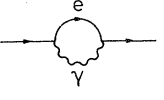
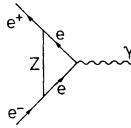
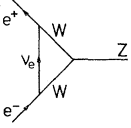
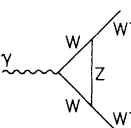
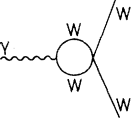
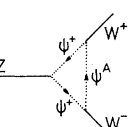
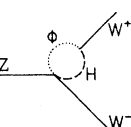
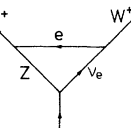
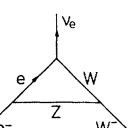
$\Sigma_{\mu\nu}^A$	t_1	20	
	t_2	2	
$\Sigma_{\mu\nu}^Z$	t_1	24	
	t_2	4	
$\Sigma_{\mu\nu}^{AZ}$	t_1	20	
	t_2	2	
$\Sigma_{\mu\nu}^W$	t_1	19	
	t_2	6	
Σ^ν	t_1	2	
Σ^e	t_1	3	

TABLE III. Vertex-correction diagrams.

	Topology	Number of diagrams	Example
$e^+e^-\gamma$	t_1	3	
e^+e^-Z	t_1	4	
γW^+W^-	t_1	26	
	t_2	10	
ZW^+W^-	t_1	31	
	t_2	10	
$e^+\nu_e W^+$	t_1	4	
$e^-\nu_e W^-$	t_1	4	

dom, are taken into account. The width of the neutral weak vector boson is also neglected.

III. KINEMATICS

In defining the kinematics for the process (see Fig. 1)

$$e^+(p_+) + e^-(p_-) \rightarrow W^+(q_+) + W^-(q_-),$$

where the momenta p_+ and p_- are taken to be incoming and q_+ and q_- to be outgoing, with [the Pauli metric $(+, +, +, +)$ is used]

$$p_+^2 = p_-^2 = 0,$$

$$q_+^2 = q_-^2 = -m_W^2$$

in the high-energy limit, the Mandelstam variables

$$s = \frac{s'}{m_W^2}, \quad s' = -(p_+ + p_-)^2,$$

$$t = \frac{t'}{m_W^2}, \quad t' = -(p_+ - q_+)^2$$

are introduced. They are equal to

$$s = \frac{E_{\text{c.m.}}^2}{m_W^2},$$

$$t = 1 - \frac{1}{2}s[1 + (1 - 4/s)^{1/2}\cos\theta_{\text{c.m.}}]$$

with $E_{\text{c.m.}}$ the center-of-mass energy and $\theta_{\text{c.m.}}$ the angle between \vec{p}_- and \vec{q}_+ . The polarization vectors of W^\pm are denoted by ϵ^\pm .

I only consider unpolarized e^+e^- beams.

IV. LOWEST ORDER

Three Feynman diagrams contribute in lowest order to the process $e^+e^- \rightarrow W^+W^-$. A photon and a neutral weak vector boson are exchanged in the s channel, while an electron neutrino is exchanged in the t channel (see Fig. 2). The expression for the tree amplitude reads

$$\begin{aligned} M_0 = (2\pi)^4 g^2 \left[\sin^2\theta_W \frac{1}{-s'} \bar{v}(p_+) \gamma_\lambda u(p_-) V_{\mu\nu\lambda}(-q_+, -q_-, q_+ + q_-) \right. \\ \left. - \cos\theta_W \frac{1}{-s' + m_Z^2} \bar{v}(p_+) \gamma_\lambda (v + a\gamma_5) u(p_-) V_{\mu\nu\lambda}(-q_+, -q_-, q_+ + q_-) \right. \\ \left. + \frac{1}{4} \frac{1}{-t'} \bar{v}(p_+) \gamma_\mu (\not{p}_- - \not{q}_-) \gamma_\nu (1 + \gamma_5) u(p_-) \right] \epsilon_\mu^+ \epsilon_\nu^- \end{aligned}$$

with g the weak coupling constant,

$$v = \frac{\sin^2\theta_W - \frac{1}{4}}{\cos\theta_W}, \quad a = -\frac{1}{4\cos\theta_W},$$

and

$$V_{\mu\nu\lambda}(k_1, k_2, k_3) = \delta_{\mu\nu}(k_1 - k_2)_\lambda + \delta_{\nu\lambda}(k_2 - k_3)_\mu + \delta_{\lambda\mu}(k_3 - k_1)_\nu.$$

The corresponding differential cross section (in mb if m_W is in GeV) is given by

$$\frac{d\sigma^0}{d\Omega} = \frac{(0.6240)^2(1 - 4/s)^{1/2}}{32\pi m_W^2 s} g^4 (d\sigma_{AA}^0 + d\sigma_{ZZ}^0 + d\sigma_{\nu\nu}^0 + d\sigma_{AZ}^0 + d\sigma_{A\nu}^0 + d\sigma_{Z\nu}^0),$$

where, for example, $d\sigma_{AZ}^0$ arises from the γZ interference. The $d\sigma^0$ are, in terms of the independent kinematical variables s and t , equal to

$$d\sigma_{AA}^0 = -2 \frac{\sin^4\theta_W}{s^2} F_1(s, t), \quad d\sigma_{ZZ}^0 = -2 \frac{(v^2 + a^2)\cos^2\theta_W}{(-s + \sec^2\theta_W)^2} F_1(s, t),$$

$$d\sigma_{\nu\nu}^0 = -\frac{1}{4} \frac{1}{t^2} F_2(s, t), \quad d\sigma_{AZ}^0 = -4 \frac{v \cos\theta_W \sin^2\theta_W}{s(-s + \sec^2\theta_W)} F_1(s, t),$$

$$d\sigma_{A\nu}^0 = \frac{\sin^2\theta_W}{st} F_3(s, t), \quad d\sigma_{Z\nu}^0 = \frac{(v+a)\cos\theta_W}{(-s + \sec^2\theta_W)t} F_3(s, t),$$

where

$$F_1(s, t) = (s^2 - 4s + 12)t^2 + (s^3 - 6s^2 + 20s - 24)t - 4s^3 + 17s^2 - 4s + 12,$$

$$F_2(s, t) = t^4 + (s - 2)t^3 - (4s - 5)t^2 + 4(s - 2)t + 4,$$

$$F_3(s, t) = (s - 2)t^3 + s(s - 4)t^2 - (4s^2 - 5s - 6)t - 8s - 4.$$

This formula agrees with the result obtained by Alles *et al.*⁶. [The lowest-order cross section (Sec. 3) of Ref. 5 contains a number of misprints and the curves of Figs. 3 and 4 should be multiplied with $(1 - 4/s)^{1/2}/(1 - 1/s)^{1/2}$. Furthermore, in (3.5) the factor β^{-2} in the equation for F_1 should be omitted, while in the equation for F_3 the factor β^{-3} must be replaced by β^{-2} .]

The total cross section (in mb if m_W is in GeV) for unpolarized e^+e^- beams in lowest order is given by

$$\sigma^0 = \frac{(0.6240)^2(1 - 4/s)^{1/2}}{128\pi m_W^2 s} g^4 (\sigma_{AA}^0 + \sigma_{ZZ}^0 + \sigma_{\nu\nu}^0 + \sigma_{AZ}^0 + \sigma_{A\nu}^0 + \sigma_{Z\nu}^0)$$

with

$$\sigma_{AA}^0 = \frac{\sin^4\theta_W}{s^2} G_1(s), \quad \sigma_{ZZ}^0 = \frac{(v^2 + a^2)\cos^2\theta_W}{(-s + \sec^2\theta_W)^2} G_1(s), \quad \sigma_{\nu\nu}^0 = G_2(s),$$

$$\sigma_{AZ}^0 = 2 \frac{v \cos\theta_W \sin^2\theta_W}{s(-s + \sec^2\theta_W)} G_1(s), \quad \sigma_{A\nu}^0 = \frac{\sin^2\theta_W}{s} G_3(s), \quad \sigma_{Z\nu}^0 = \frac{(v+a)\cos\theta_W}{-s + \sec^2\theta_W} G_3(s),$$

where

$$G_1(s) = \frac{2}{3}s(s^3 + 16s^2 - 68s - 48),$$

$$G_2(s) = \frac{1}{12}(s^2 + 20s - 48) + 4 \left[1 - \frac{2}{s} \right] \frac{1}{(1 - 4/s)^{1/2}} \ln \frac{1 + (1 - 4/s)^{1/2}}{1 - (1 - 4/s)^{1/2}},$$

$$G_3(s) = -\frac{1}{3}(s^3 + 18s^2 - 28s - 24) + 32 \left[1 + \frac{1}{2s} \right] \frac{1}{(1 - 4/s)^{1/2}} \ln \frac{1 + (1 - 4/s)^{1/2}}{1 - (1 - 4/s)^{1/2}}.$$

Again this formula agrees with results obtained by various authors.⁶⁻⁸

V. ONE-LOOP CORRECTIONS

Radiative corrections for scattering processes⁹ consist of two parts: virtual corrections, due to closed loops in Feynman diagrams, and real corrections caused by the bremsstrahlung of photons. The differential cross section for $e^+e^- \rightarrow W^+W^-$ to order g^6 can be expressed in the form

$$\frac{d\sigma}{d\Omega} = \frac{d\sigma^0}{d\Omega} (1 + \delta_T)$$

with δ_T the total radiative correction. It is then composed of two terms

$$\delta_T = \delta_V + \delta_B,$$

where δ_V is the contribution of the virtual corrections, i.e., the contribution from the interference

between the three lowest-order diagrams and the ones in which one closed loop occurs, and δ_B is the bremsstrahlung correction, due to the emission of a photon which escapes detection. The virtual correction is equal to

$$\delta_V = \delta_s + \delta_v + \delta_b + \delta_r.$$

In here δ_s denotes the contribution of the self-energy insertions, while δ_v comes from the various vertex corrections and δ_b from the box diagrams. Finally δ_r contains the renormalization counter-terms.

The complications arising from substitutions of variables, reduction of strings and evaluation of traces of Dirac γ matrices, etc., are considerable. To this end extensive use has been made of the algebraic-manipulation program REDUCE.¹⁰

In computing one-loop Feynman graphs, one has to evaluate in the dimensional regularization scheme integrals of the following type:

$$T(m^2) = \int d^n q \frac{1}{q^2 + m^2} ,$$

$$S_{0,\mu,\nu}(k^2, m_1^2, m_2^2) = \int d^n q \frac{1, q_\mu, q_\nu}{(q^2 + m_1^2)[(q+k)^2 + m_2^2]} ,$$

$$V_{0,\mu,\nu,\nu\lambda}(k_1^2, k_2^2, (k_1+k_2)^2, m_1^2, m_2^2, m_3^2) = \int d^n q \frac{1, q_\mu, q_\nu, q_\lambda}{(q^2 + m_1^2)[(q+k_1)^2 + m_2^2][(q+k_1+k_2)^2 + m_3^2]} ,$$

$$B_{0,\mu,\nu,\nu\lambda,\nu\lambda\sigma}(k_1^2, k_2^2, k_3^2, (k_1+k_2)^2, (k_2+k_3)^2, (k_1+k_2+k_3)^2, m_1^2, m_2^2, m_3^2, m_4^2) \\ = \int d^n q \frac{1, q_\mu, q_\nu, q_\lambda, q_\sigma}{(q^2 + m_1^2)[(q+k_1)^2 + m_2^2][(q+k_1+k_2)^2 + m_3^2][(q+k_1+k_2+k_3)^2 + m_4^2]} .$$

Every such one-loop integral can be decomposed in terms of form factors. Take for example $V_{\mu\nu}$ (depending on six Lorentz invariants):

$$V_{\mu\nu} = V_1^2 \delta_{\mu\nu} + V_2^2 k_\mu^1 k_\nu^1 + V_3^2 k_\mu^2 k_\nu^2 + V_4^2 k_\mu^1 k_\nu^2$$

with $k_{\mu\nu}^1 = k_\mu^1 k_\nu^2 + k_\nu^1 k_\mu^2$. These 64 one-loop form factors are algebraically related to the scalar integrals T , S_0 , V_0 , and B_0 ,¹¹ for which 't Hooft and Veltman derived exact analytical expressions (in terms of logarithms and Spence functions).¹² The complete set of formulas has been programmed into a long program, called FOLFFGT, for the evaluation of all dimensionally regularized one-loop form factors.¹³

In this section I will discuss the one-loop virtual corrections to $e^+e^- \rightarrow W^+W^-$ in some more detail.

(i) *Self-energy diagrams* (see Fig. 3 and Table II). Many graphs, of two different types, namely without (t_1) and with four-vertices (t_2), contribute to the photon and neutral-weak-vector-boson self-energies $\Sigma_{\mu\nu}^A$ and $\Sigma_{\mu\nu}^Z$ and to the photon—neutral-weak-vector-boson mixing $\Sigma_{\mu\nu}^{AZ}$. Their contributions to the cross section are, respectively, proportional to $\Delta_1^A(-s')$, $\Delta_1^Z(-s') - \Delta_1^Z(-m_Z^2)$, and $\Delta_1^{AZ}(-s')$ with

$$\Sigma_{\mu\nu}(k^2) = \Delta_1(k^2) \delta_{\mu\nu} + \Delta_2(k^2) k_\mu k_\nu .$$

The contribution due to the electron-neutrino self-energy Σ^ν is further proportional to $\Delta^\nu(-t')$ with

$$\Sigma^\nu(k^2) = \frac{1}{2} \Delta^\nu(k^2) (1 - \gamma_5) \not{k} .$$

The wave-function renormalization of the charged weak vector bosons is also determined by their self-energy $\Sigma_{\mu\nu}^W$. Again two types of graphs contribute. The renormalized W^\pm wave functions are equal to

$$\left[1 + \frac{1}{2} g^2 \frac{\partial \Delta_1^W}{\partial k^2} \right]_{k^2 = -m_W^2} \epsilon^\pm .$$

Finally writing the electron (positron) self-energy as

$$\Sigma^e(k^2) = i [\Delta_1^e(k^2) - \Delta_2^e(k^2) \gamma_5] \not{k} + \Delta_3^e(k^2) m_e ,$$

the renormalized e^\pm wave functions are given by their free spinors multiplied with

$$1 + \frac{1}{2} g^2 \left[\Delta_1^e(-m_e^2) - 2m_e^2 \left[\frac{\partial \Delta_1^e}{\partial k^2} \right]_{k^2 = -m_e^2} - \frac{\partial \Delta_3^e}{\partial k^2} \right]_{k^2 = -m_e^2} + \frac{1}{2} g^2 \Delta_2^e(-m_e^2) .$$

Note that the electron is taken to be massive. I also checked the Slavnov-Taylor identities for the various vector-boson self-energies.

(ii) *Vertex-correction diagrams* (see Fig. 4 and Table III). A large number of graphs contribute to the corrections to the $e^+e^- \gamma$, $e^+e^- Z$, $\gamma W^+ W^-$, $Z W^+ W^-$, $e^+ \nu_e W^+$, and $e^- \nu_e W^-$ vertices.

Again two different topologies (t_1 and t_2) can be distinguished. The three-vector-boson vertex corrections are free of anomalies, because quark loop are also taken into account.

(iii) *Box diagrams* (see Fig. 5 and Table IV). The box graphs can be divided into three different classes, namely the direct (t_1), crossed (t_1) and tri-

angular (t_2) box graphs. Their contribution δ_b to the cross section is given by their interference with the three lowest-order diagrams.

VI. RENORMALIZATION

The one-loop virtual corrections are in general ultraviolet divergent. In order to remove these divergencies, appearing in the dimensional regularization scheme as terms containing

$$I = \frac{2}{n-4} + \ln\pi - \gamma$$

with n the number of space-time dimensions and γ Euler's constant, counterterms have to be added to the Lagrangian. In QFD it is enough to renormalize three free parameters, for example, the electromagnetic coupling constant, the weak mixing angle, and the mass of the charged weak vector bosons. Therefore, one needs three experimental data. The electromagnetic fine-structure constant and the weak mixing angle¹⁴ are equal to

$$\alpha = \frac{e^2}{4\pi} = \frac{1}{137.04}, \quad \sin^2\theta_W = 0.23,$$

so that, using a lowest-order relation, the weak fine-structure constant equals

$$\beta = \frac{g^2}{4\pi} = \frac{e^2}{4\pi \sin^2\theta_W} = \frac{1}{31.52}.$$

The value of the mass of the charged weak vector bosons is, however, not yet known. I take

$$m_W = 80.33 \text{ GeV}$$

and

$$m_Z = 91.54 \text{ GeV}.$$

These numbers are very near to the one-loop-corrected values calculated by Antonelli *et al.*,¹⁵ but they still satisfy the lowest-order relation

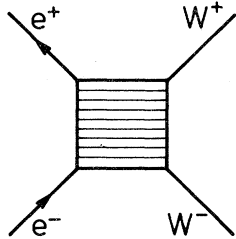


FIG. 5. Box diagrams.

TABLE IV. Box diagrams.

Topology	Number of diagrams	Example
Direct t_1	13	
Crossed t_1	13	
Triangular t_2	5	

$$\frac{m_W}{m_Z} = \cos\theta_W.$$

The renormalization δe^2 of the electric charge can be determined by computing the one-loop

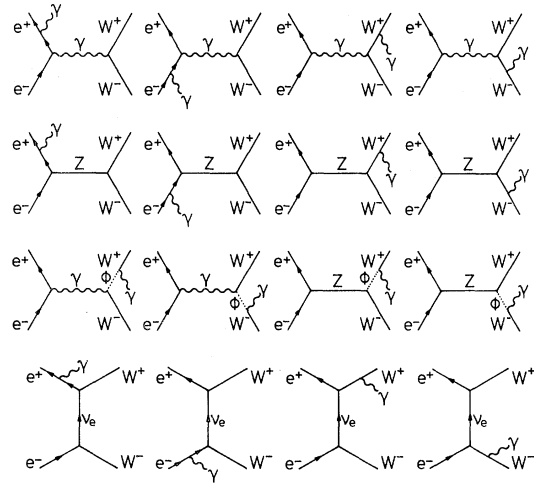


FIG. 6. Diagrams for $e^+e^- \rightarrow W^+W^-\gamma$.

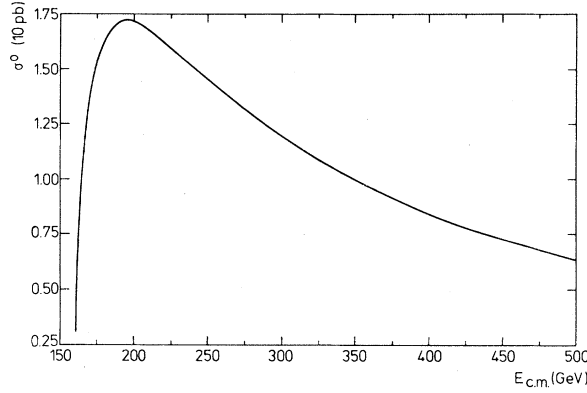


FIG. 7. The lowest-order total cross section for $e^+e^- \rightarrow W^+W^-$.

corrections to Coulomb scattering of muons on electrons. This has also been done by Antonelli *et al.*¹⁵ and I use their result. The renormalization of the weak-vector-boson masses is further fixed by their self-energies, namely,

$$\delta m_W^2 = \Delta_1^W(-m_W^2), \quad \delta m_Z^2 = \Delta_1^Z(-m_Z^2),$$

so that the renormalization of the weak mixing angle is given by the formula

$$\delta \sin^2 \theta_W = \frac{\cos^2 \theta_W \delta m_Z^2 - \delta m_W^2}{m_Z^2}.$$

The contribution from the counterterm Lagrangian

$$\delta \mathcal{L}_{\text{QFD}} = \mathcal{L}_{\text{QFD}}(e + \delta e, \sin \theta_W + \delta \sin \theta_W, m_W + \delta m_W) - \mathcal{L}_{\text{QFD}}(e, \sin \theta_W, m_W)$$

to the cross section is then equal to

$$\left[\delta e^2 \frac{\partial}{\partial e^2} + \delta \sin^2 \theta_W \frac{\partial}{\partial \sin^2 \theta_W} \right] \frac{d\sigma^0}{d\Omega}.$$

TABLE V. The lowest-order total cross section for $e^+e^- \rightarrow W^+W^-$ for different values of the center-of-mass energy.

$E_{c.m.}$ (GeV)	$\sigma^0(10^3 \text{ pb})$
165	1.02
175	1.54
200	1.71
225	1.60
250	1.45
350	1.00
500	0.63

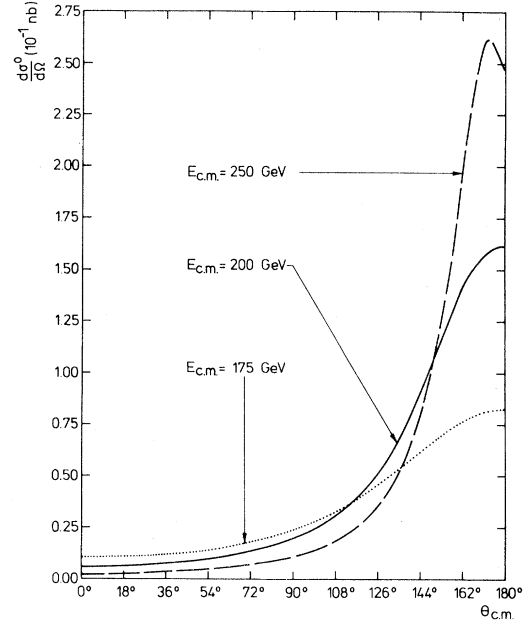


FIG. 8. The lowest-order differential cross section for $e^+e^- \rightarrow W^+W^-$ for some values of the center-of-mass energy.

The total virtual correction now turns out to be ultraviolet finite, as expected in a renormalizable theory.

VII. BREMSSTRAHLUNG

Finally there are the infrared divergencies of the one-loop virtual corrections. These infinities, regu-

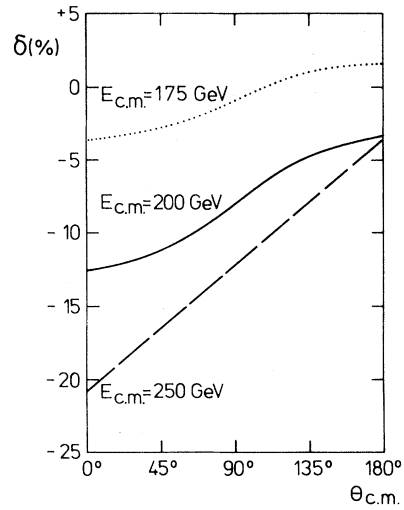


FIG. 9. The percentage one-loop radiative corrections to the lowest-order differential cross section for $e^+e^- \rightarrow W^+W^-$ for a Higgs-boson mass of 100 GeV and for some values of the center-of-mass energy.

TABLE VI. The lowest-order differential cross section for $e^+e^- \rightarrow W^+W^-$ in 10^{-1} nb for different values of the center-of-mass energy and the scattering angle.

$\theta_{c.m.}$ $E_{c.m.}$ (GeV)	0°	18°	36°	54°	72°	90°	108°	126°	144°	162°	180°
175	0.106	0.110	0.123	0.147	0.185	0.243	0.331	0.458	0.619	0.770	0.832
200	0.061	0.065	0.078	0.100	0.137	0.198	0.307	0.513	0.889	1.406	1.619
250	0.023	0.026	0.035	0.049	0.071	0.108	0.183	0.355	0.797	1.973	2.467
500	0.001	0.002	0.004	0.008	0.012	0.018	0.033	0.074	0.209	0.942	3.511

larized by introducing a small fictitious photon mass λ , are canceled by the soft-real-photon bremsstrahlung contribution. Therefore, the Feynman diagrams of Fig. 6 have to be evaluated. Owing to a Slavnov-Taylor identity for the lowest-order amplitude, the bremsstrahlung cross section factorizes into an infrared factor

$$\delta_B = \frac{\sin^2 \theta_W}{16\pi^3} g^2 \times \int_{|\vec{k}| < \chi} \frac{d\vec{k}}{(\vec{k}^2 + \lambda^2)^{1/2}} \left[\frac{p_+}{k \cdot p_+} - \frac{p_-}{k \cdot p_-} - \frac{q_+}{k \cdot q_+} + \frac{q_-}{k \cdot q_-} \right]^2$$

with k the photon four-momentum and into the lowest-order cross section $d\sigma^0/d\Omega$. This infrared integral has been worked out previously by 't Hooft and Veltman.¹² Also here the mass of the electron cannot be neglected. I take the threshold energy E_{th} at which the charged weak vector bosons can be detected equal to $0.45 E_{c.m.}$, so that the cutoff is given by⁹

$$\chi = \frac{E_{c.m.}^2}{20[0.55E_{c.m.} + (0.2025E_{c.m.}^2 - m_W^2)^{1/2}]}$$

TABLE VII. The percentage one-loop radiative corrections to the lowest-order differential cross section for $e^+e^- \rightarrow W^+W^-$ at a center-of-mass energy $E_{c.m.}$ of 175 GeV for different values of the Higgs-boson mass and the scattering angle.

m_H (GeV)	$\theta_{c.m.}$	0°	45°	90°	135°	180°
25		-5.54	-4.86	-2.98	-1.09	-0.38
100		-3.57	-2.85	-0.95	+0.95	+1.67
750		+0.03	+0.79	+2.71	+4.62	+5.35

VIII. RESULTS

There are very strong cancellations between the different contributions to the lowest-order total cross section for $e^+e^- \rightarrow W^+W^-$. This is characteristic for gauge theories. The cross section, of the order of 10 pb, rises sharply and attains not far above threshold its maximum (17.2 pb at $E_{c.m.} = 195$ GeV), from where on it decreases slowly. Numerical results are given in Table V and plotted in Fig. 7.

The lowest-order differential cross section, of the order of 10^{-1} nb, is very asymmetric: it is strongly peaked near $\theta_{c.m.}$ equal to 180° . This effect gets more pronounced at higher energies (at $E_{c.m.} = 500$ GeV the cross section almost reaches 1 nb). The electron-neutrino exchange is responsible for this peaking. It was, however, pointed out by Gaemers and Gounaris that it is possible to eliminate the neutrino-exchange contribution by using polarized beams.⁷ Numerical results are listed in Table VI and plotted in Fig. 8.

The percentage one-loop radiative corrections to the lowest-order angular distribution are found to be negative, except in the case of low energy, and they increase considerably in going from 175 to 500 GeV. The percentage corrections decrease while, because of the peaking of the cross section, the absolute corrections increase with growing scattering angles. I calculated the corrections for different values of the Higgs-boson mass ($m_H = 25, 100$, and 750 GeV). The dependence on that mass

TABLE VIII. Same as Table VII with $E_{c.m.} = 200$ GeV.

m_H (GeV)	$\theta_{c.m.}$	0°	45°	90°	135°	180°
25		-14.27	-12.82	-9.63	-6.44	-4.99
100		-12.62	-11.17	-7.98	-4.79	-3.34
750		-9.63	-8.18	-4.99	-1.80	-0.35

TABLE IX. Same as Table VII with $E_{\text{c.m.}} = 250$ GeV.

m_H (GeV)	$\theta_{\text{c.m.}}$	0°	45°	90°	135°	180°
25		-22.54	-18.13	-13.78	-9.46	-5.15
100		-20.83	-16.54	-12.25	-7.96	-3.68
750		-17.89	-13.73	-9.50	-5.24	-0.98

is about 5%, so that, in order to see the effect of the Higgs particle, very accurate measurements of the cross section are required. Note finally that the corrections at $E_{\text{c.m.}} = 175$ GeV have a different sign for small and large Higgs-boson mass. Numerical results for the percentage corrections are presented in Tables VII–X and plotted in Fig. 9. The relative behavior of the one-loop corrections for various energies and Higgs-boson masses is nearly the same as that of Ref. 5. The shifts in magnitude are probably a consequence of the adoption of a different, but related, renormalization procedure and the use of smaller quark masses.

IX. CONCLUSIONS

In this work I presented the cross section for $e^+e^- \rightarrow W^+W^-$ up to the one-loop level within

TABLE X. Same as Table VII with $E_{\text{c.m.}} = 500$ GeV.

m_H (GeV)	$\theta_{\text{c.m.}}$	0°	45°	90°	135°	180°
25		-52.05	-37.99	-29.56	-21.18	-7.23
100		-50.06	-36.16	-27.81	-19.47	-5.56
750		-46.32	-32.57	-24.31	-16.01	-2.14

the framework of quantum flavor dynamics. Experimental confirmation of the theoretical prediction will be crucial for the validity of the non-Abelian gauge idea.

ACKNOWLEDGMENTS

I would like to thank R. Gastmans for suggesting this work, for continuous interest and stimulating discussions. I am further grateful to J. Prentki for his hospitality at the CERN theory division, where part of the calculation was performed, and also to M. Veltman for clarifying discussions. Finally, I acknowledge the financial support of the Nationaal Fonds voor Wetenschappelyk Onderzoek (Belgium).

APPENDIX

The QFD Feynman rules are easily derived from the Lagrangian, neglecting Higgs-boson–fermion couplings and quark mixings,

$$\begin{aligned}
\mathcal{L}_{\text{QFD}} = & -\frac{1}{2}A_{\mu,\nu}A_{\mu,\nu} - \frac{1}{2}Z_{\mu,\nu}Z_{\mu,\nu} - \frac{1}{2}\frac{1}{c^2}m_W^2Z_\mu Z_\mu - W_{\mu,\nu}^+W_{\mu,\nu}^- - m_W^2W_\mu^+W_\mu^- \\
& -\frac{1}{2}H_{,\mu}H_{,\mu} - \frac{1}{2}m_H^2H^2 - \frac{1}{2}\Phi_{,\mu}^0\Phi_{,\mu}^0 - \frac{1}{2}\frac{1}{c^2}m_W^2\Phi^0\Phi^0 - \Phi_{,\mu}^+\Phi_{,\mu}^- - m_W^2\Phi^+\Phi^- \\
& -isg(A_{\mu,\nu}W_\mu^{[+}W_\nu^{-]} - A_\nu W_\mu^{[+}W_{\mu,\nu}^{-]} + A_\mu W_\nu^{[+}W_{\mu,\nu}^{-]} - icg(Z_{\mu,\nu}W_\mu^{[+}W_\nu^{-]} - Z_\nu W_\mu^{[+}W_{\mu,\nu}^{-]} + Z_\mu W_\nu^{[+}W_{\mu,\nu}^{-]}) \\
& -s^2g^2(A_\mu A_\mu W_\nu^+W_\nu^- - A_\mu W_\mu^+A_\nu W_\nu^-) - c^2g^2(Z_\mu Z_\mu W_\nu^+W_\nu^- - Z_\mu W_\mu^+Z_\nu W_\nu^-) \\
& -scg^2[2A_\mu Z_\mu W_\nu^+W_\nu^- - A_\mu Z_\nu(W_\mu^+W_\nu^- + W_\nu^+W_\mu^-)] \\
& -\frac{1}{2}g^2W_\mu^+W_\mu^-W_\nu^+W_\nu^- + \frac{1}{2}g^2W_\mu^+W_\nu^-W_\mu^+W_\nu^- + \frac{1}{2}m_H^2m_W^2g^{-2} - 2\omega m_W^2g^{-2} \\
& -2\omega m_Wg^{-1}H - \frac{1}{2}\omega[H^2 + (\Phi^0)^2 + 2\Phi^+\Phi^-] - \frac{1}{4}\frac{m_H^2}{m_W}gH[H^2 + (\Phi^0)^2 + 2\Phi^+\Phi^-] \\
& -\frac{1}{32}\frac{m_H^2}{m_W^2}g^2[H^4 + (\Phi^0)^4 + 2H^2(\Phi^0)^2 + 4H^2\Phi^+\Phi^- + 4(\Phi^0)^2\Phi^+\Phi^- + 4(\Phi^+\Phi^-)^2]
\end{aligned}$$

$$\begin{aligned}
& -\frac{1}{2} \frac{1}{c^2} m_W g Z_\mu Z_\mu H - m_W g W_\mu^+ W_\mu^- H + i s m_W g A_\mu (W_\mu^+ \Phi^- - W_\mu^- \Phi^+) - i \frac{s^2}{c} m_W g Z_\mu (W_\mu^+ \Phi^- - W_\mu^- \Phi^+) \\
& + \frac{1}{2} \frac{1}{c} g Z_\mu (H \Phi_{,\mu}^0 - \Phi^0 H_{,\mu}) + i s g A_\mu (\Phi^+ \Phi_{,\mu}^- - \Phi^- \Phi_{,\mu}^+) + i \frac{c^2 - \frac{1}{2}}{c} g Z_\mu (\Phi^+ \Phi_{,\mu}^- - \Phi^- \Phi_{,\mu}^+) \\
& + \frac{1}{2} g [W_\mu^+ (H \Phi_{,\mu}^- - \Phi^- H_{,\mu}) + W_\mu^- (H \Phi_{,\mu}^+ - \Phi^+ H_{,\mu})] \\
& - \frac{1}{2} i g [W_\mu^+ (\Phi^0 \Phi_{,\mu}^- - \Phi^- \Phi_{,\mu}^0) - W_\mu^- (\Phi^0 \Phi_{,\mu}^+ - \Phi^+ \Phi_{,\mu}^0)] \\
& - s^2 g^2 A_\mu A_\mu \Phi^+ \Phi^- - \frac{1}{8} \frac{1}{c^2} g^2 Z_\mu Z_\mu [H^2 + (\Phi^0)^2 + 8(s^2 - \frac{1}{2})^2 \Phi^+ \Phi^-] - 2 \frac{s}{c} (c^2 - \frac{1}{2}) g^2 A_\mu Z_\mu \Phi^+ \Phi^- \\
& - \frac{1}{4} g^2 W_\mu^+ W_\mu^- [H^2 + (\Phi^0)^2 + 2 \Phi^+ \Phi^-] + \frac{1}{2} i s g^2 A_\mu H (W_\mu^+ \Phi^- - W_\mu^- \Phi^+) - \frac{i}{2} \frac{s^2}{c} g^2 Z_\mu H (W_\mu^+ \Phi^- - W_\mu^- \Phi^+) \\
& + \frac{1}{2} s g^2 A_\mu \Phi^0 (W_\mu^+ \Phi^- + W_\mu^- \Phi^+) - \frac{1}{2} \frac{s^2}{c} g^2 Z_\mu \Phi^0 (W_\mu^+ \Phi^- + W_\mu^- \Phi^+) \\
& - \bar{\nu}_l \partial \nu_l - \bar{l} (\partial + m_l) l - \bar{q}_c^\dagger (\partial + m_{q^\dagger}) q_c^\dagger - \bar{q}_c^\dagger (\partial + m_{q_l}) q_c^\dagger - i s g A_\mu (\bar{l} \gamma_\mu l - \frac{2}{3} \bar{q}_c^\dagger \gamma_\mu q_c^\dagger + \frac{1}{3} \bar{q}_c^\dagger \gamma_\mu q_c^\dagger) \\
& + \frac{i}{4} \frac{1}{c} g Z_\mu [\bar{\nu}_l \gamma_\mu (1 + \gamma_5) \nu_l + \bar{l} \gamma_\mu (4s^2 - 1 - \gamma_5) l + \bar{q}_c^\dagger \gamma_\mu (-\frac{8}{3} s^2 + 1 + \gamma_5) q_c^\dagger + \bar{q}_c^\dagger \gamma_\mu (\frac{4}{3} s^2 - 1 - \gamma_5) q_c^\dagger] \\
& + \frac{1}{2\sqrt{2}} i g W_\mu^+ [\bar{\nu}_l \gamma_\mu (1 + \gamma_5) l + \bar{q}_c^\dagger \gamma_\mu (1 + \gamma_5) q_c^\dagger] + \frac{1}{2\sqrt{2}} i g W_\mu^- [\bar{l} \gamma_\mu (1 + \gamma_5) \nu_l + \bar{q}_c^\dagger \gamma_\mu (1 + \gamma_5) q_c^\dagger] \\
& + \bar{\Psi}^A \partial^2 \Psi^A + \bar{\Psi}^0 \left[\partial^2 - \frac{1}{c^2} m_W^2 \right] \Psi^0 + \bar{\Psi}^+ (\partial^2 - m_W^2) \Psi^+ + \bar{\Psi}^- (\partial^2 - m_W^2) \Psi^- \\
& + i s g A_\mu (\bar{\Psi}_{,\mu}^+ \Psi^+ - \bar{\Psi}_{,\mu}^- \Psi^-) + i c g Z_\mu (\bar{\Psi}_{,\mu}^+ \Psi^+ - \bar{\Psi}_{,\mu}^- \Psi^-) \\
& - i s g [W_\mu^+ (\bar{\Psi}_{,\mu}^+ \Psi^A - \bar{\Psi}_{,\mu}^A \Psi^-) - W_\mu^- (\bar{\Psi}_{,\mu}^- \Psi^A - \bar{\Psi}_{,\mu}^A \Psi^+)] - i c g [W_\mu^+ (\bar{\Psi}_{,\mu}^+ \Psi^0 - \bar{\Psi}_{,\mu}^0 \Psi^-) - W_\mu^- (\bar{\Psi}_{,\mu}^- \Psi^0 - \bar{\Psi}_{,\mu}^0 \Psi^+)] \\
& - \frac{1}{2} m_W g H \left[\frac{1}{c^2} \bar{\Psi}^0 \Psi^0 + \bar{\Psi}^+ \Psi^+ + \bar{\Psi}^- \Psi^- \right] + \frac{1}{2} i m_W g \Phi^0 (\bar{\Psi}^+ \Psi^+ - \bar{\Psi}^- \Psi^-) - i s m_W g (\Phi^+ \bar{\Psi}^+ \Psi^A - \Phi^- \bar{\Psi}^- \Psi^A) \\
& - i \frac{c^2 - \frac{1}{2}}{c} m_W g (\Phi^+ \bar{\Psi}^+ \Psi^0 - \Phi^- \bar{\Psi}^- \Psi^0) + \frac{i}{2} \frac{1}{c} m_W g (\Phi^+ \bar{\Psi}^0 \Psi^- - \Phi^- \bar{\Psi}^0 \Psi^+) ,
\end{aligned}$$

where $c = \cos \theta_W$, $s = \sin \theta_W$, $x_{,\mu} = \partial_\mu x$, and $x^{[a} y^{b]} = x^a y^b - x^b y^a$. The factor ω must be adjusted so that the sum of the Higgs-boson tadpole diagram contributions is equal to zero.

¹See, e.g., E. S. Abers and B. W. Lee, Phys. Rep. **9C**, 1 (1973); L. D. Faddeev and A. A. Slavnov, *Gauge Fields: Introduction to Quantum Theory* (Benjamin, New York, 1980).

²G. 't Hooft, Nucl. Phys. **B35**, 167 (1971).

³S. L. Glashow, Nucl. Phys. **22**, 579 (1961); S. Weinberg, Phys. Rev. Lett. **19**, 1264 (1967); A. Salam, in *Elementary Particle Theory: Relativistic Groups and Analyticity* (Nobel Symposium No. 8), edited by N. Svartholm (Almqvist and Wiksell, Stockholm, 1968),

- p. 367; S. L. Glashow, J. Iliopoulos, and L. Maiani, Phys. Rev. D **2**, 1285 (1970).
- ⁴CERN Report No. CERN/ISR-LEP/79-33, 1979 (unpublished).
- ⁵M. Lemoine and M. Veltman, Nucl. Phys. **B164**, 445 (1980).
- ⁶W. Alles, Ch. Boyer, and A. J. Buras, Nucl. Phys. **B119**, 125 (1977).
- ⁷K. J. F. Gaemers and G. J. Gounaris, Z. Phys. C **1**, 259 (1979).
- ⁸O. P. Sushkov, V. V. Flambaum, and I. B. Khriplovich, Yad. Fiz. **20**, 1016 (1974) [Sov. J. Nucl. Phys. **20**, 537 (1975)]; F. Bletzacker and H. T. Nieh, Nucl. Phys. **B124**, 511 (1977); R. W. Brown and K. O. Mikaelian, Phys. Rev. D **19**, 922 (1979).
- ⁹F. A. Berends, K. J. F. Gaemers, and R. Gastmans, Nucl. Phys. **B57**, 381 (1973); **B63**, 381 (1973); F. A. Berends and R. Gastmans, in *Electromagnetic Interactions of Hadrons*, edited by A. Donnachie and G. Shaw (Plenum, New York, 1978).
- ¹⁰A. C. Hearn, REDUCE 2 User's Manual, University of Utah, 1973 (unpublished).
- ¹¹G. Passarino and M. Veltman, Nucl. Phys. **B160**, 151 (1979).
- ¹²G. 't Hooft and M. Veltman, Nucl. Phys. **B153**, 365 (1979).
- ¹³R. Philippe, FOLFFGT, a FORTRAN program for the evaluation of all dimensionally regularized one-loop form factors in gauge theories, Leuven, 1981 (unpublished).
- ¹⁴J. E. Kim, P. Langacker, M. Levine, and H. H. Williams, Rev. Mod. Phys. **53**, 211 (1981).
- ¹⁵F. Antonelli, G. Corbo, M. Consoli, and O. Pellegrino, Nucl. Phys. **B183**, 195 (1981).